SINERGI Vol. 30, No. 2, June 2026: 469-480
http://publikasi.mercubuana.ac.id/index.php/sinergi
http://doi.org/10.22441/sinergi.2026.2.013

Taguchi-based optimization of activation parameters in activated carbon production for water pollutant adsorption

I Gusti Agung Kade Suriadi[1,2], Dewa Ngakan Ketut Putra Negara[3]*, Tjokorda Gde Tirta Nindia[3], I Ketut Adi Atmika[3], I Gusti Komang Dwijana[3], I Made Gatot Karohika[3], Anak Agung Istri Agung Sri Komaladewi[2], Gopi Prasetiyo[3]

[1]Doctoral Study Program of Engineering Science, Faculty of Engineering, Udayana University, Indonesia
[2]Industrial Engineering Department, Faculty of Engineering, Udayana University, Indonesia
[3]Mechanical Engineering Department, Faculty of Engineering, Udayana University, Indonesia

Abstract

Water pollution from synthetic dyes, particularly methylene blue (MB), is known to pose serious environmental and public health challenges. Therefore, among various treatment methods, adsorption using activated carbon remained the most cost-effective and energy-efficient. In this research, activated carbon was prepared from Petung bamboo (Dendrocalamus asper), with the Taguchi method used to optimize the activation parameters. The following three factors: activation temperature (700°C, 800°C), holding time (40 min, 80 min), and activating gas (N_2, CO_2) were investigated based on an $L_4(2^3)$ orthogonal array design. The characterization process included proximate analysis, functional group identification, amorphous structure determination, and surface morphology examination. Optimization using the larger-is-better signal-to-noise (SN) ratio model aimed to maximize methylene blue adsorption. Additionally, analysis of variance (ANOVA) showed that activating gas, holding time, and temperature contributed 48.69%, 34.86%, and 8.06%, respectively, to adsorption performance, and all three parameters had a statistically significant influence on methylene blue adsorption. The optimal conditions, namely 800°C activation temperature, 40 min holding time, and N_2 gas, produced a maximum adsorption capacity of 9.275 mg/g. As a result, these findings showed that activated carbon derived from Petung bamboo was a sustainable and renewable adsorbent, offering a promising pathway toward environmentally friendly and cost-effective wastewater treatment technologies.

Keywords:
Activation;
Adsorption;
Dyes;
Optimization;
Taguchi;

Article History:
Received: June 15, 2025
Revised: October 22, 2025
Accepted: October 31, 2025
Published: June 6, 2026

Corresponding Author:
Dewa Ngakan Ketut Putra Negara
Mechanical Engineering Department, Faculty of Engineering, Udayana University, Indonesia.
Email: devputranegara@unud.ac.id

INTRODUCTION

Water contamination from synthetic dyes, including methylene blue (MB), is a serious global environmental issue. These dyes are commonly used across various industries, such as textiles [1], pharmaceuticals, and chemicals, which significantly affect water quality, thereby disrupting aquatic ecosystems. Methylene blue is particularly of great concern due to its inability to break down easily [2], implying it persists in the environment, constituting a serious hazard to both human health and aquatic life. The negative impact includes potential cancer risks and interference with photosynthesis in aquatic organisms [3]. Managing this pollution requires the creation of efficient and environmentally responsible solutions, particularly for treating wastewater that contains dangerous compounds. Several methods for removing dyes and other pollutants have been explored, such as advanced oxidation processes [4], membrane filtration [5], photocatalytic degradation [6], and adsorption [7].

Among these methods, adsorption is particularly appealing due to the cost-effectiveness, as well as the availability of both natural and engineered adsorbents, namely biochar-derived carbon and clay-based materials [8]. Furthermore, adsorption is a relatively straightforward method that uses minimal energy, making it a great option for wastewater treatment.

Activated carbon is another relevant material for treating wastewater, specifically in getting rid of synthetic dyes such as methylene blue. The impressive ability to adsorb contaminants was derived from its well-developed microporous structure, large surface area, and significant pore volume [9], low ash content, and reactive surface chemistry. The different functional groups on the surface strengthened its capacity to adsorb a wide range of pollutants upon interaction [10]. However, the use of commercially available activated carbon was often constrained by the production costs, mainly arising from the dependence on non-renewable resources such as coal, lignite, polymers, and petroleum by-products that are becoming scarce [11]. This led to a growing interest in finding low-cost, sustainable materials, including biomass, such as coconut shells [12] and bamboo [13].

Bamboo is a great source of activated carbon because of its high carbon content, rapid growth, and naturally porous structure. In addition, this structure helps form both micro- and mesopores during activation. Several studies reported that bamboo-derived activated carbon had strong potential when using chemical and physical activation methods. For example, previous research stated that bamboo activated with KOH and H_3PO_4 effectively removed impurities, opened up pores, as well as improved surface area and adsorption capacity [14]. Nitrogen (N_2)-activated thorny bamboo carbon showed excellent absorption performance for heavy metals, including cadmium (Cd), mercury (Hg), and lead (Pb) [15]. These results supported the selection of bamboo, specifically Petung.

Petung bamboo (*Dendrocalamus asper*) has shown significant potential due to its high cellulose and lignin content, rapid growth, and abundance, particularly in tropical regions such as Indonesia [16]. Compared to other biomasses, it offered a competitive edge in terms of carbon yield, ease of processing, and environmental impact. The structural properties made it suitable for conversion into activated carbon through dehydration, carbonization, and activation stages [17].

Numerous studies have reported the complex interdependence between relevant variables, namely holding time, activation temperature, and steam flow, making it difficult to optimize related parameters for biomass-derived activated carbon [18]. In this context, activation temperature had a major effect on the pore structure of activated carbon. At low temperatures, specific surface area and pore volume might not reach their best levels due to the incomplete decomposition of raw materials. Extremely high activation temperature could lead to the collapse of the pore structure, while those in the range of 600-900°C were used to produce activated carbon from thorny bamboo [15], with temperatures of 700 and 800°C serving as benchmarks. Supposing the holding time is brief, it might not form optimal pores, and when the duration is lengthy, the activation temperature could raise production costs without yielding significant benefits.

Other parameters, such as the type of activating gas, greatly affected the physicochemical characteristics of activated carbon, including pore size distribution, surface morphology, and adsorption capacity [11]. Gas-based activators, namely carbon dioxide (CO_2) and N_2, were often used in physical activation because of the capability of forming uniform microscopic pores. N_2 is an inert gas that acts as a protective atmospheric layer during carbonization to prevent oxidation and maintain the stability of the carbon structure. Meanwhile, CO_2 reacts with carbon at high temperatures, forming pores, as well as increasing the surface area and adsorption capacity. These parameters interact in complex ways to influence the microporosity and mesoporosity of the resulting activated carbon. The insights reinforced the need for structured optimization methods such as Taguchi, aimed to enhance efficiency and reproducibility in activated carbon analyses.

In this context, Taguchi was selected due to the ability to generate an efficient experimental design using fewer trials than other methods, namely full factorial or Response Surface Methodology (RSM). Additionally, the method saved both time and money. In recent years, it has evolved as a powerful and efficient statistical tool for optimizing process parameters in the production of activated carbon. This method enabled the effective design of experiments using a reduced number of trials, which led to reliable parameter estimation while minimizing time, cost, and resource consumption. Apart from its efficiency, the Taguchi method helped to identify the most influential factors affecting the performance of activated carbon, particularly adsorption capacity. Several research had applied this method successfully to optimize

conditions for activated carbon derived from various biomass sources, such as coconut [19], leading to enhanced adsorption capacities, including improved overall process efficiency. Furthermore, Taguchi focused on creating strong designs against variation or noise, as well as aiming to obtain the best average value. The use of orthogonal arrays and signal-to-noise (SN) ratio analysis made it simple to identify the most relevant factors without requiring complex statistical skills.

Considering the proven benefits, no prior research had used the Taguchi method to simultaneously evaluate the effects of activating gas, temperature, and holding time on activated carbon produced from Petung bamboo, specifically for methylene blue dye removal. This present research addressed the gap by systematically applying the Taguchi method to optimize the critical parameters. The method is entirely eco-friendly, as the activation process does not use any chemical activating agents, thereby minimizing environmental impact. The objective is to enhance the adsorption performance of Petung bamboo–based activated carbon, as well as support the development of sustainable and environmentally benign materials. This also included advancing efficient wastewater treatment technologies, scaled for real-world applications.

METHOD

Material

Petung bamboo, collected from Baturiti Village, Tabanan, Bali, Indonesia, served as the precursor in this experiment. Based on earlier research, the chemical composition of this material constituted 37.33% cellulose, 28.69% lignin, and 19.35% hemicellulose [16]. CO_2 and N_2 gases used during the activation process were acquired from PT Samabayu Mandala, a gas supplier with headquarters in Mengwi, Badung, Bali. Furthermore, the Udayana University Analytical Laboratory provided the model dye, methylene blue, used in the adsorption experiment.

Methods

A flowchart was designed to ensure the research model provided a detailed explanation of biomass transformation, Taguchi optimization, and adsorption evaluation. Meanwhile, reproducibility and clarity were increased by a visual flowchart of the entire procedure, from raw material preparation to characterization, methylene blue adsorption test, and optimization, as in Figure 1. Table 1 shows a thorough analysis of L_4 (2^3) orthogonal array.

Bamboo was first sliced into small pieces, thoroughly cleaned with distilled water, and allowed to dry for five days under the sun. It was subsequently dried at 105°C in an electrical furnace until the weight was constant. The dried bamboo was further subjected to heat in an electric furnace at 750°C and in a reactor regulated at a rate of 10°C per minute to carbonize the product. Based on the efficacy, as reported by previous research, this precise rate was selected [20]. After reaching the proper temperature, it was held for half an hour before being allowed to cool at room temperature in the furnace. Uniform particle size was obtained by ensuring the resultant biochar was ground into fine powder and sieved using a 60-mesh sieve.

The activation procedure, as shown in Table 1, was determined by the factors in each row.

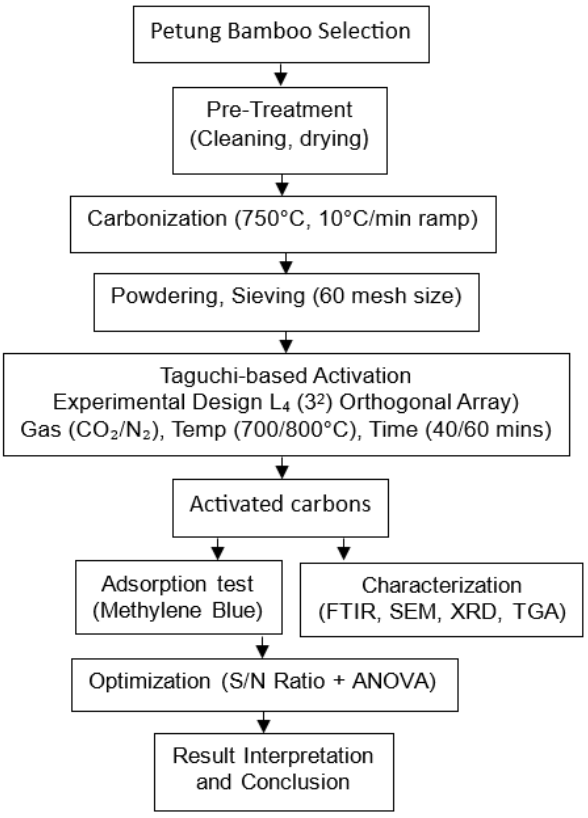

Figure.1. Experiment procedure

Table 1. Experimental design, $L_4(2^3)$

Running	Factors (Independent variable) and levels		
	Factor A Activation temperatures	Factor B Activation holding times	Factor C Activators gases
L1	700°C-level 1	60 min-level 1	CO_2-level 1
L2	700°C-level 1	80 min-level 2	N_2-level 2
L3	800°C-level 2	40 min-level 1	N_2-level 2
L4	800°C-level 2	80 min-level 2	CO_2-level 1

Furthermore, in the first experiment (L1), CO_2 was the gas used, including the activation temperature and time of 700°C and 40 minutes, respectively.

The precise procedure was reported as follows: the activation reactor was filled with 50 grams of charcoal. The reactor placed in an electrical furnace was heated to 700°C and held at the same temperature for 40 minutes, with CO_2 flowing continuously at a rate of 200 mL/min. Subsequently, the reactor was allowed to cool to room temperature. The sample was taken out of the reactor and put in an airtight container immediately it reached room temperature. The subsequent tests (L2, L3, and L4) were carried out following the same process, using the relevant factor levels in Table 1, where N_2 flow rate applied was also 200 mL/min. In accordance with experiment orders L1, L2, L3, and L4, activated carbon samples were designated as AC-RL1, AC-RL2, AC-RL3, and AC-RL4.

Optimization was performed using the larger-the-better criteria to obtain an adequate amount of activated carbon adsorption on the methylene blue. The ideal combination of parameters was represented by the highest SN ratio, which was used to determine the optimal level of each factor [19]. SN ratio for the larger-the-better criteria was calculated using (1) [21]. In this case, n denotes the number of repetitions, and y_i represents the performance or response that was measured.

$$SNR = -10\,log\left(\frac{1}{n}\sum_{i=1}^{n}\frac{1}{y_i^2}\right) \quad (1)$$

The impact and contribution of each factor were quantitatively examined using analysis of variance (ANOVA).

Characterization

Numerous characterizations, such as proximate testing, FTIR (Fourier transform infrared spectroscopy), SEM (scanning electron microscopy), and XRD (X-ray diffraction) tests (with scan range theta, speed and Cu Kα of 10-90, 0.02 deg/min, and= 1.5406, respectively), were carried out to analyze activated carbon. The proximate composition of activated carbon was assessed by conducting proximate tests using a Thermogravimetric Analyzer (TGA 701-Biomass ASTM D7582 MVA). Additionally, SEM-JSM-6510LA was used to analyze the surface morphology of activated carbon. The IRPrestige-21 test instrument with 2 cm^{-1} resolution was adopted during FTIR experiments to evaluate the functional groups of activated carbon. This also led to the use of the PANalytical X'Pert PRO apparatus to perform an XRD test in order to observe the amorphous structure.

Methylene blue adsorption test

Batch adsorption experiments were carried out to evaluate the adsorption performance of activated carbon toward methylene blue. Prior to analysis, the UV-visible spectrophotometer was calibrated using a series of methylene blue standard environments (0–12 ppm) to generate a calibration curve (R^2 > 0.997), which ensured accurate quantification of methylene blue residual concentration. During each experiment, 20 milliliters of 5 ppm methylene blue solution (pH 5.64) was mixed with 0.1 g of activated carbon. Additionally, bias was minimized by ensuring all experiments were performed randomly under the same stirring conditions of 100 rpm for 20 minutes. After 20 minutes of constant stirring, the suspension was allowed to stand for 3 hours before being filtered. Measurement of the amount of methylene blue remaining in the filtrate was performed using a wavelength of 664 nm [22]. Adsorption capacity (q_e) was computed using (2) [23].

$$q_e = \frac{(C_o - C_e)V}{W} \quad (2)$$

where C_o and C_e denoted the initial and final concentrations of methylene blue (mg/L), V represented the solution volume (L), and W depicted the mass of activated carbon used (g). Data reliability and consistency were ensured by performing experiments in triplicate.

RESULTS AND DISCUSSION

Proximate analysis

Proximate composition of activated carbon in Table 2 is in the ranges of 9.01% to 10.72%, 11.90% to 15.09%, 4.28% to 8.01%, and 69.37% to 72.23% for moisture, volatile matter, ash content, and fixed carbon content, respectively. The sample containing the highest amount of fixed carbon content was activated carbon AC-RL3. However, the sample with the lowest was AC-RL4. For adsorption purposes, a high fixed carbon content was considered beneficial when combined with low levels of ash, moisture, and volatile matter.

Table 2. Proximate composition of samples

Activated carbons	Composition of proximate elements (%)			
	Moisture	Volatile	Ash	Fixed carbon
AC-RL1	9.01	15.09	4.28	71.62
AC-RL2	9.67	13.87	5.70	70.76
AC-RL3	9.58	12.38	5.81	72.23
AC-RL4	10.72	11.90	8.01	69.37

Considering the proximate composition of activated carbon samples did not differ significantly, all formulations satisfied the Indonesian National Standard (SNI 06-3730-1995). This regulation stipulated that the ash content must not exceed 10%, the fixed carbon content should be a minimum 65%, the maximum moisture content equivalent to 15%, and the volatile matter less than 25%.

FTIR analysis

FTIR spectroscopy was used to identify the functional groups present in activated carbon samples. The results of the analysis were shown in Figure 2. Meanwhile, Table 3 describes the detected functional groups along with the corresponding wavenumbers. Virtually all samples, except AC-RL2, exhibited hydroxyl (O-H) functional groups in the wavenumber range of 3718.92–3843.33 cm^{-1}. These hydroxyl groups, composed of oxygen and hydrogen atoms [24], enhanced the interaction of carbon with aqueous environments.

All activated carbon samples showed aliphatic C-H stretching vibrations of approximately 2300 cm^{-1}. The presence of C=C functional groups was also observed in all samples in the wavenumber range of 1508.4–1538.3 cm^{-1}. These functional groups were formed through structural transformations during the carbonization and activation processes, leading to the development of aromatic rings in an amorphous graphitic matrix [25]. The presence of C=C bonds in the rings enhanced the structural stability and adsorption efficiency of the material. The diverse characteristics contributed significantly to the performance of activated carbon. Generally, the occurrence of these functional groups showed the material's strong potential for use in various environmental cleanup efforts and industrial adsorption or filtration applications.

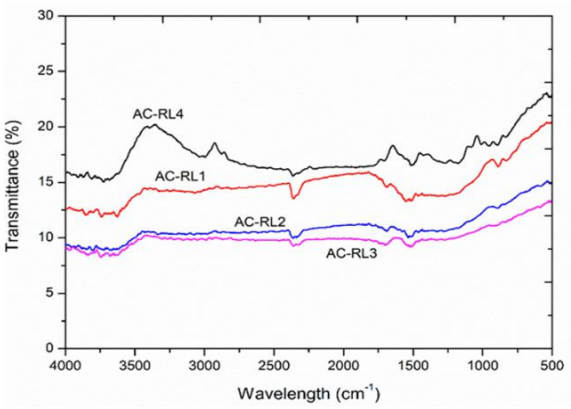

Figure 2. FTIR analysis

Table 3. The wavenumber and functional groups detected in activated carbon

Activated carbons	Peaks (cm^{-1})				
AC-RL1	3843.33		2347.47	1538.30	888.26
AC-RL2			2348.43	1523.83	
AC-RL3	3840.44		2342.65	1523.83	
AC-RL4	3718.92	3011.95	2352.29	1508.40	
Functional groups	O-H Hydroxyl stretching	C-H Alkenes (Strtch)	C-H Aliphatic stretching	C=C Aromatic	C-H Aromatic (bend)

XRD analysis

The structural characteristics and degree of amorphousness of activated carbon samples were evaluated using XRD analysis. This method included observing the diffraction patterns produced when X-rays interacted with the atomic structure of a material. Moreover, it was commonly used to distinguish between crystalline and amorphous phases in carbon-based substances. The resulting diffraction patterns in Figure 3, showed weak and broad peaks, particularly within the 2θ ranges of 10–30° and 40–45°. The crystallinity index values were calculated using Origin software, which provided additional insight into the degree of structural ordering. These broad reflections depicted a predominantly amorphous carbon structure with limited long-range atomic order. The absence of sharp and intense peaks, typically associated with well-organized crystalline carbon forms, depicted the disordered nature of the carbon lattice. As an alternative, the observed patterns conformed to the turbostratic arrangement, where carbon layers were randomly stacked and rotationally uneven. This structural disorder was consistent with earlier research that reported broad diffuse peaks of approximately 2θ ≈ 23° and 43°, characteristic of an amorphous or poorly ordered carbon matrix [26]. The broadness of the peaks was attributed to the presence of microstructural defects and short-range ordering in graphitic microdomains, often introduced during the carbon activation process.

This observation was consistent with the results of the crystallinity index (CI), calculated to be 40.89% (AC-RL1), 53.69% (AC-RL2), 53.15% (AC-RL3), and 54.93% (AC-RL4). The values implied that the structure contained locally ordered areas or tiny graphitic domains. The predominance of broad diffraction peaks suggested that the structure was mainly amorphous. Despite the existence of certain crystalline fractions, weak and diffuse diffraction reflections were caused by the small size and presence of microstructural defects.

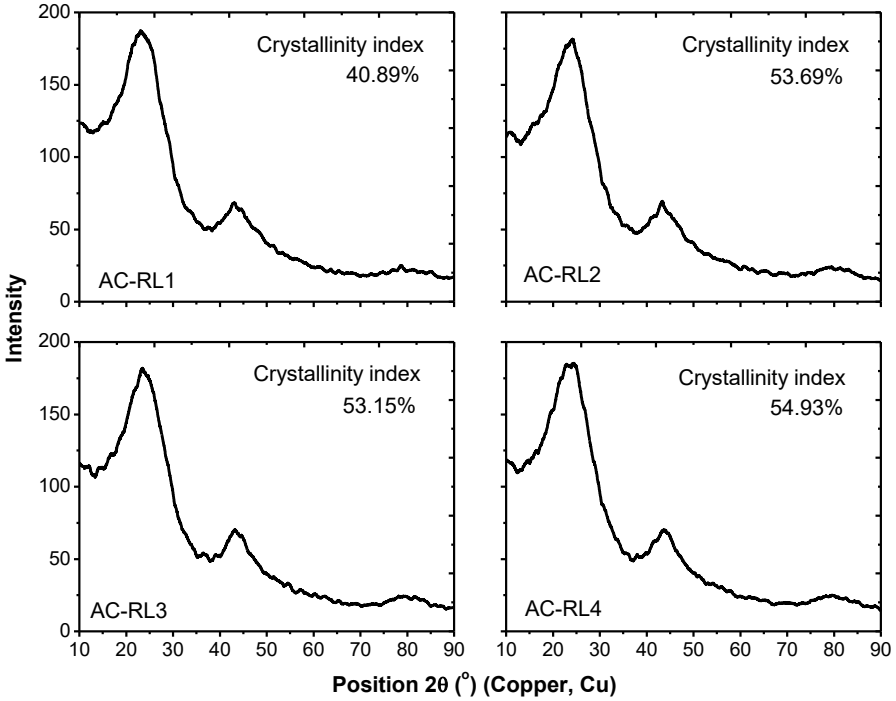

Figure 3. X-ray diffraction test results of the sample

These mixed structures were typical of activated carbons obtained through physical or chemical methods. The predominance of amorphous regions was advantageous for adsorption-based applications because it provided a larger surface area and more accessible active sites [27]. Therefore, both the XRD patterns and crystallinity index data showed that the produced activated carbon exhibited a predominantly amorphous microstructure with limited crystalline domains. The amorphous nature significantly influenced the efficiency and effectiveness of the material, resulting in its suitability for diverse industrial and environmental uses. Regarding the circumstance, adsorption played a significant role in performance, such as during filtration, purification, and pollutant removal processes.

Surface morphology

Figure 4 shows the surface characteristics of activated carbon samples. These depicted activated carbon had a rough, uneven surface with amorphous, porous particles, regarded as morphological features that were advantageous for adsorption applications. The successful execution of the carbonization and activation processes was supported by the existence of a well-developed porous structure. The activated carbon structure in the AC-RL1 sample was characterized by big, rough-textured pores. This was because CO_2 acted as the activating gas, causing a gasification reaction that increased the size of the pores. However, the complete development of pores was limited by the comparatively short activation period of 40 minutes.

The AC-RL2 sample had fewer macropores and more evenly spaced, smaller pores. As an inert gas, N_2 preserved the integrity of the carbon structure rather than actively creating pores. Meanwhile, increasing the holding time to 80 minutes improved structural stability, which had minimal effect on the development of larger pores. The combination of small and medium-sized pores enabled the AC-RL3 sample to possess a more porous structure. The pyrolysis process was significantly enhanced by increasing the activation temperature to 800°C, which facilitated the formation of a well-developed porous structure. In particular, the AC-RL4 sample exhibited a highly complex morphology characterized by abundant macropores and mesopores. This porous network was mainly attributed to the synergistic effect of high-temperature treatment and CO_2 activation, which contributed to the development of a large surface area.

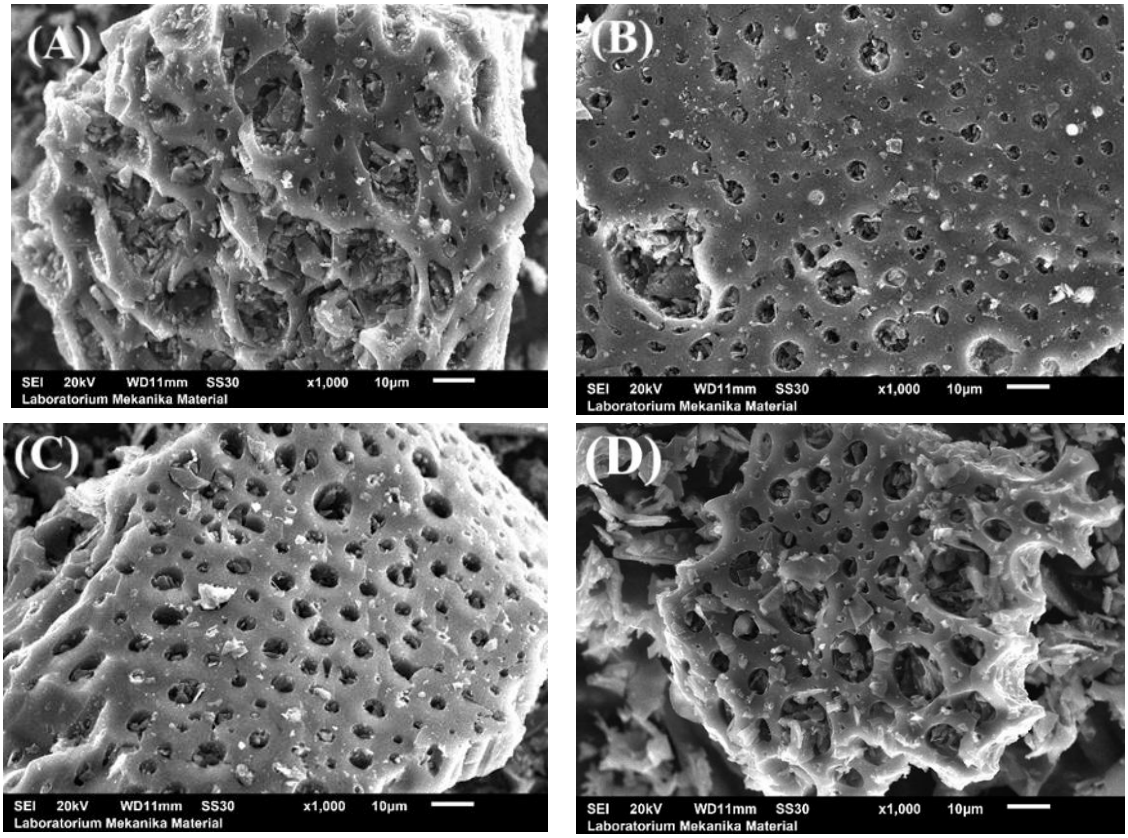

Figure 4. SEM image of samples. (A) = AC-RL1, (B) = AC-RL2, (C) = AC-RL3, and (D) = AC-RL4

However, extending the holding time to 80 minutes potentially promoted pore development and also introduced the risk of partial structural collapse. Under extreme conditions, CO_2 enlarged micropores into mesopores, which reduced the overall adsorption efficiency. This was due to the loss of optimal microporous characteristics, typically more favorable for certain adsorption processes [28].

Optimization analysis

Table 4 shows the experimental data for methylene blue adsorption that were assessed by applying the Taguchi method and calculated using Minitab software. The adoption of the larger-is-better criteria enabled the calculation of SN ratios for different levels of parameters A, B, and C, as shown in Table 5. The distinct SN ratio of levels 1 and 2 in each factor showed that the delta values was equivalent to the differences between the highest and lowest SN ratios for each parameter. The relative impact of each factor on the response was also shown in Figure 5. The delta values of 0.82, 0.69, and 0.31, for parameters C, B, and A, respectively, proved that parameter C was ranked as having the most significant impact on adsorption performance, followed by B and A. Data gathered showed the best condition for optimizing adsorption capacity was Level 2 of parameter C (18.85), which produced the highest SN ratio. The further support of the role in improved adsorption performance was that Levels 1 and 2 of parameters B and A, respectively, correlated with higher SN ratios.

Based on these results, enhancing the adsorption process required optimizing parameter C, with B and A having a comparatively smaller effect. The significance of the parameters in system optimization for increased performance and efficiency was supported by the fact that parameter C was the most important factor in reaching a higher SN ratio, followed by B and A. The optimal condition was represented by the highest adsorption value at each factor level since the optimization depended on the larger-is-better criteria. Moreover, this condition was accomplished with N_2 activator (C1), carbonization holding time of 40 minutes (B1), and activation temperature of 800°C (A2).

Table 4. The experiment results of methylene blue adsorption, average, and standard deviation

Activated carbons	Factors and levels			Methylene blue adsorbed (mg/g)				
	A Activation Temperatures (°C)	B Holding times (minutes)	C Activator gases	1	2	3	Average	Standard deviation
AC-RL1	700	40	CO_2	8.397	8.098	7.958	8.151	0.244
AC-RL2	700	80	N_2	8.036	8.489	8.297	8.274	0.227
AC-RL3	800	40	N_2	9.252	9.440	9.134	9.275	0.154
AC-RL4	800	80	CO_2	7.558	7.936	7.906	7.800	0.210

Table 5. Response SN ratio

Level	A	B	C
1	18.28	18.78	18.03
2	18.59	18.09	18.85
Delta	0.31	0.69	0.82
Rank	3	2	1

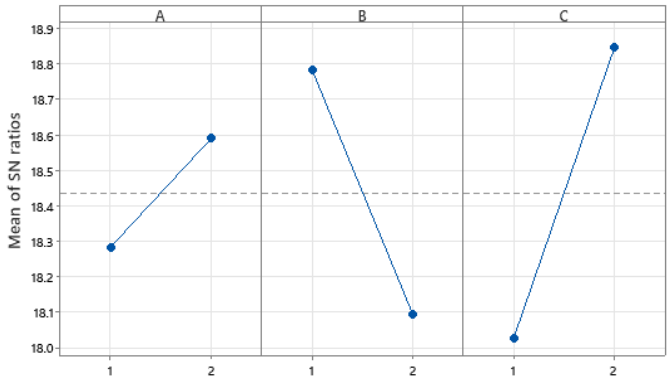

Figure 5. Main effects plot for SN ratios (larger is better) of data means

Table 6. ANOVA

Source	DF	Seq SS	Contribution	Adj SS	Adj MS	F-Value	P-Value	F-Table
A	1	0.3172	8.06%	0.3172	0.3172	7.69	0.024	5.71
B	1	1.3716	34.86%	1.3716	1.3716	33.24	0.000	
C	1	1.9160	48.69%	1.9160	1.9160	46.43	0.000	
Error	8	0.3301	8.39%	0.3301	0.0412			
Total	11	3.9340	100.00%					

Table 6 shows an overview of ANOVA used to assess the significance of factor influence and its contribution to methylene blue adsorption. SN ratio was used in ANOVA rather than the raw mean, because the method penalized variation in results, rather than poor average values, combining performance and robustness aspects. The method also combined the main objective of Taguchi, which aimed to reduce the sensitivity of the process to uncontrolled variation. The evaluation was conducted using the F test [29], which compared the F table with the calculated F. The P-test compared the P-value with a specific level of significance [30]. The three degrees of freedom and a total of 12 samples ensured that the computation of the F-table value, at a significance level of 2.5%, was 5.71. Moreover, every factor had a significant impact on the adsorption of methylene blue, as evidenced by the fact that all computed F-values were greater than the F-table. The results supported the idea that every factor had a significant impact, with all P-values less than the 2.5% significance level. The proposed model was dependable and exhibited slightly unexplained variability, with a comparatively low error rate of 8.39%. The percentage contributions of each factor were as follows, from the highest to the lowest factors C (48.69%), B (34.86%), and A (8.06%).

Considering that the activator influenced the porosity and surface structure of the activated material, it had a greater impact on the activation process than the holding time and temperature. The type of activator directly affected pore formation and microstructural development by dictating the main chemical reactions that occurred during activation. During interactions with the raw material, activators such as N_2 and CO_2 exhibited unique reaction mechanisms. The activator played an essential role in the formation of microstructures [31], while holding time and temperature were mainly used to maximize its conditions. The final material properties were directly and significantly affected by changes in the activator, with temperature and time variations refining the created conditions.

In this context, N_2 was proven to be a more potent activator than CO_2, using Petung bamboo as the raw material. The outcome was explained by the unique activation mechanism of each gas. CO_2 promoted activation through gasification ($C + CO_2 \rightarrow 2CO$), which led to the creation of bigger and less uniform pores [28]. N_2, as an inert gas, triggered the formation of a more uniform microstructure by reducing excessive reactions and increasing total pore surface area. These results were in line with the surface morphology shown in Figure 4.

Comparison with Prior Research

The results showed a maximum methylene blue adsorption capacity of 9.275 mg/g under ideal conditions (activation temperature of 800°C, holding time of 40 minutes, and activating gas N_2). These were consistent with the results of previous international analyses. Steam-activated carbon made from palm kernel shell exhibited a comparable adsorption performance, with a maximum capacity of 14.7 mg/g based on the Langmuir isotherm [32]. The dosage of the adsorbent had a significant impact on the adsorption capacity of methylene blue. Furthermore, adsorption capacity per unit mass of the adsorbent (Q_e) tended to decrease with increasing doses, because site saturation and particle agglomeration restricted the effective surface area. This behavior explained the reason behind the dependency on the exact dose administered, and Q_e values frequently falling between 10 mg/g and 24 mg/g [33]. The physical activation methods supported environmentally friendly practices by avoiding the use of chemical agents. Both results showed that physically activated carbons produced moderate methylene blue uptake, typically below, around, or just slightly above 20 mg/g [33]. However, the absolute adsorption capacities differed due to variations in raw materials, activation media, and surface characteristics.

An earlier research found that activated carbon with superior textural qualities, such as a high BET surface area and micropore volume of 1491.75 m^2/g and 0.5813 cm^3/g, respectively, was produced by activation at 800°C with a 1:3 KOH impregnation ratio [34]. Another research reported that the ideal activation conditions for generating activated carbon from Honduran mahogany pod husk were 800°C for 30 minutes, producing a BET surface area and total pore volume of 966 m^2/g and 0.43 cm^3/g [35]. The consistent activation temperature used in these analyses outlined the relevance of 800°C as an ideal threshold for improving surface characteristics and adsorption efficiency in carbon materials derived from biomass. The consistency in holding time between 30 and 40 minutes proved how effective this thermal window triggered the formation of porous structures conducive to high adsorption capacity.

Considering that this research did not obtain BET surface area data, the comparison with earlier analyses remained relevant. The adsorption capacity of methylene blue served as an indirect measure of surface area and pore development. Since the adsorption process mainly occurred on the surface and in mesopores, its uptake clearly reflected the adsorption performance and surface features of activated carbon. However, the absence of BET analysis was a limitation, as it restricted the direct quantification of surface area and pore volume. Quantitative comparison with other biomass precursors was acknowledged to provide additional context. This research mainly focused on optimizing the activation parameters for Petung bamboo to evaluate the intrinsic potential. Comparative analysis with other biomass precursors was outside the current scope and should be considered in future work. Regardless of these limitations, the results provided valuable insight into the adsorption potential of Petung bamboo–based activated carbon, which could be further explored for removing other organic and inorganic pollutants in aqueous systems.

In comparison with previous research, the adsorption capacity of 9.275 mg/g achieved was moderate. However, this result supported the main objective of the research to develop an environmentally friendly and resource-efficient activation process, rather than to maximize adsorption capacity through chemical modification. Compared to chemical activation methods that often use corrosive agents such as KOH or H_3PO_4, physical activation with CO_2 and N_2 gases was used in this context. These gases

were cleaner, non-toxic, and easier to handle. The choice minimized environmental impact and production costs. Adsorption performance achieved was not regarded as a limitation, it reflected a more sustainable process that avoided hazardous chemicals and produced activated carbon with satisfactory adsorption potential. This method showed the possible conversion of Petung bamboo, a renewable and fast-growing biomass, into functional activated carbon through an eco-friendly method. Additionally, the method proved that sustainability and adsorption performance were effectively balanced.

CONCLUSION

In conclusion, the adsorption efficiency of activated carbon for the removal of methylene blue was significantly influenced by the type of activating gas, temperature, and holding time. N_2 outperformed CO_2 among the gases examined in terms of producing a consistent and fully formed pore structure. An 800°C temperature and a 40-minute holding period were found to be the ideal activation conditions. The highest recorded adsorption capacity for methylene blue was obtained by combining N_2, with a temperature and holding period of 800°C, and a 40-minute holding period, respectively. The results outlined the significance of selecting appropriate activation conditions in order to maximize the performance and environmental resilience of activated carbon. These provided a strong basis for further research focused on the scaling up of activation processes by applying the optimized carbon materials to real wastewater treatment systems, particularly in industries that discharge dye-laden effluents. Future research should examine the generated capacity of activated carbon for regeneration and reuse purposes, as well as the effective removal of other organic and inorganic pollutants in a range of environmental settings.

ACKNOWLEDGMENT

The authors gratefully acknowledge the financial support provided for this study under the Leading Research of Study Program initiative, as stated in contract number B/255.162/UN14.4.A/PT.01.03/2024. This funding was made available by the Research and Community Service Institute (LPPM) of Udayana University through the Faculty of Engineering.

REFERENCES

[1] I. Khan et.al, “Review on Methylene Blue: Its properties, uses, toxicity and photodegradation,” *Wate*r, vol. 14, no. 242, pp. 2-30, January 2022, doi: 10.3390/w14020242

[2] P. Sharma, M. Ganguly, and M. Sahu,“ Photocatalytic degradation of methyl blue dye with H_2O_2 sensing,” *RSC Advances*, vol. 14, pp. 14606-14615, 2024, doi: 10.1039/d4ra01354a

[3] J. Fito et al., “Adsorption of methylene blue from textile industrial wastewater using activated carbon developed from Rumex abyssinicus plant,” *Scientific Report*, vol. 13, no. 5427, pp. 1-17, 2023, doi: 10.1038/s41598-023-32341-w

[4] S. Ledakowicz and K. Pazdzior, “Recent achievements in dyes removal focused on advanced oxidation processes integrated with biological methods,” *Molecules*, vol. 26, no. 870, pp. 1-45, February 2021, doi: 10.3390/molecules26040870

[5] H. Türe, “Adsorption of methylene blue dye onto alginate-bioglass membranes: response surface method, isotherm, and kinetic studies,” Gumushane *University Journal of Science*, vol. 13, no. 3, pp. 538–552, 2023, doi: 10.17714/gumusfenbil.1245309

[6] Z. S. Khalifa and M. Shaban, “Photocatalytic degradation of methyl orange and methylene blue dyes by engineering the surface nano-textures of TiO_2 thin films deposited at different temperatures via MOCVD,” *Molecules*, vol. 28, no. 3, pp. 1-13, January 2023, doi: 10.3390/molecules28031160

[7] R. Erlangga, D. A. Sari, and A. Wahyuningtyas, “Characterization of Eichhornia crassipes bio-adsorbent activated by H_3PO_4 for the removal of lead ion (Pb^{2+}) from wastewater of battery industry,” *SINERGI*, vol. 29, no. 2, pp. 279–286, June 2025, doi: 10.22441/sinergi.2025.2.002

[8] J. Hayfron, S. Jaaskelainen, and S. Tetteh, “Synthesis of zeolite from rice husk ash and kaolinite clay for the removal of methylene blue from aqueous solution,” Heliyon, vol. 11, no. 1, pp. 1-14, January 2025, doi: 10.1016/j.heliyon.2024.e41325

[9] D. Bosch et.al, “Alternative feedstock for the production of activated carbon with $ZnCl_2$: Forestry residue biomass and waste wood,” *Carbon Resources Conversion*, vol. 5, no. 4, pp. 299–309, 2022, doi: 10.1016/j.crcon.2022.09.001

[10] M. K. Jha et al., “Surface modified activated carbons : sustainable bio-based materials for environmental remediation,” *Nanomaterials*,

vol. 11, no. 11, pp. 1–20, November 2021, doi: 10.3390/nano11113140

[11] P. C. Bhomick, "Pine Cone biomass as an efficient precursor for the synthesis of activated biocarbon for adsorption of anionic dye from aqueous solution: Isotherm, kinetic, thermodynamic and regeneration studies," Sustainable *Chemistry and Pharmacy*, vol. 10, pp. 41–49, December 2018, doi: 10.1016/j.scp.2018.09.001

[12] S. Hena, K. S. Patil, N. Leinecker, T. Bhatelia, and M. Shah, "Effect of algal organic matter on adsorption of glyphosate using coconut shell-activated carbon," *Chem. Eng. J. Adv*., vol. 22, p. 100754, April 2025, doi: 10.1016/j.ceja.2025.100754

[13] Y. Guo, D. Lu, Z. Wang, and Q. Wang, "Promising application of waste bamboo biomass-derived carbon for efficient ibuprofen removal from aqueous systems," *Environmental Technology & Innovation*, vol. 37, pp. 1–15, January 2025, doi: 10.1016/j.eti.2025.104025

[14] E. T. Suryandari, A. Syazwani, and A. Keyon, "Characterization of Indonesian bamboo charcoal for enhanced adsorption capabilities," *Walisongo Journal of Chemistry*, vol. 6, no 1, pp. 80-86, 2023, doi: 10.21580/wjc.v6i1.16158

[15] P. Huang and J. Wen, "Study on thorny bamboo activated carbon for capturing heavy metals in groundwater," Applied Mechanics and Materials, vol. 535, pp. 427–431, 2014, doi: 10.4028/www.scientific.net/AMM.535.427

[16] D. N. K. P. Negara et.al, "Characteristics evaluation of three Balinese bamboos as precursor of activated carbon," *Proceedings of the 7th International Conference on Materials Engineering and Nanotechnology 2023*, Kuala Lumpur, Malaysia 4th-5th November 2023, vol. 2, pp. 44–53, doi: 10.1007/978-981-97-4080-2_4

[17] D. Jo et.al, "Effect of pore characteristics of biomass-derived activated carbon for automobile canisters via chemical stabilization method on butane adsorption characteristics," *Technologies*, vol. 13, no. 89, pp. 1-18, February 2025, doi: 10.3390/technologies13030089

[18] D. Bergna et.all, "Effect of some process parameters on the main properties of activated carbon produced from peat in a lab-scale process," *Waste and Biomass Valorization*, vol. 11, pp. 2837–2848, 2020, doi: 10.1007/s12649-019-00584-2

[19] D.P. Kumar et.al, "Process optimization and synthesis of activated carbon from coconut shell using phosphoric acid," *Poll Res*., vol. 41, no. 2, pp. 402-405, 2022, doi: 10.53550/PR.2022.v41i02.047

[20] D. N. K. Putra Negara et al., "The effect of carbonisation heating rates on the properties of N-doped teak sawdust waste activated carbon," *Journal of Physical Science*, vol. 34, no. 3, pp. 1–20, 2023, doi: 10.21315/jps2023.34.3.1

[21] H. Arpan and K. Upendra, "Application of Taguchi methodology in adsorption of malachite green dye using chemically enhanced bambusa tulda (Indian Timber Bamboo)," *Advances in Environmental Technology*, vol. 9, no. 2, pp. 99–111, 2023, doi: 10.22104/aet.2023.5907.1622

[22] M. A. Mackinder, K. Wang, and Q. H. Fan, "Methylene blue adsorption by plasma re-activated carbon," *Journal of Water Resource and Protection*, vol 13, pp. 778–793, 2021, doi: 10.4236/jwarp.2021.1310041.

[23] A. H. Jawad et al., "Microporous activated carbon developed from KOH activated biomass waste: surface mechanistic study of methylene blue dye adsorption," *Water Science & Technology*, vol. 84, no. 8, pp. 1858–1872, 2021, doi: 10.2166/wst.2021.355.

[24] Q. Wan and B. C. Thompson, "Control of properties through hydrogen bonding interactions in conjugated polymers," *Advanced Science*, vol. 11, pp. 1–26, 2023, doi: 10.1002/advs.202305356

[25] F. Raheel et al., "Synthesis and characterization of activated carbon and its application for wastewater treatment," *Materials Proceedings*, vol. 17, no. 4, pp. 1–5, 2024, doi: 10.3390/materproc2024017004

[26] N. Ivanichok et.al, "Effect of thermal activation on the structure and electrochemical properties of carbon material obtained from walnut shells Nataliia," *Materials*, vol. 17, no. 11, pp. 1–21, 2024, doi: 10.3390/ma17112514

[27] T. W. Chew et al., "A review of bio-based activated carbon properties produced from different activating chemicals during chemicals activation process on biomass and its potential for Malaysia," *Materials*, vol. 16, no. 23, pp. 1-15, 2023, doi: 10.3390/ma16237365

[28] K. Phothong, C. Tangsathitkulchai, and P. Lawtae, "The analysis of pore development and formation of surface functional groups in bamboo-based activated carbon during CO_2 activation," *Molecules*, vol. 26, no. 18, pp. 1-26, 2021, doi: 10.3390/molecules26185641

[29] F. Abdullahu et.al, "An experimental analysis of Taguchi-based gray relational analysis, weighted gray relational analysis, and data envelopment analysis ranking method multi-criteria decision-making approaches to multiple-quality characteristic optimization in the CNC drilling process," *Processes*, vol. 12, no. 6, pp. 1-17, 2024, doi: 10.3390/pr12061212

[30] C. Waghmare, S. Patil, and P. Chaudhari, "Application of Taguchi method, ANOVA analysis, and TOPSIS technique in optimization of process parameters for surface roughness and material removal rate in electrochemical machining of Al-SiC MMCs," *Indian Journal of Science and Technology*, vol. 17, no. 16, pp. 1633–1642, 2024, doi: 10.17485/IJST/v17i16.751

[31] O. Togibasa et.al, "The effect of chemical activating agent on the properties of activated carbon from sago waste," *Applied Sciences*, vol. 11, no. 24, 2021, doi: 10.3390/app112411640

[32] K. A. M. Said et al.," Methylene blue adsorption mechanism onto palm kernel shell-derived activated carbon: From particle diffusion to site adsorption," *BioResources,* vol. 8, no. 3, pp. 5120-5132, 2023, doi: 10.15376/biores.18.3.5120-5132

[33] J. Wang, J. Ma, and Y. Sun, "Adsorption of methylene blue by coal-based activated carbon in high-salt wastewater," *Water*, vol. 14, no. 3576, pp. 1–18, 2022, doi: 10.3390/w14213576

[34] W. Thongpat, J. Taweekun, and K. Maliwan, "Synthesis and characterization of microporous activated carbon from rubberwood by chemical activation with KOH," *Carbon Lett*., vol. 31, pp. 1079-1088, 2020, doi: 10.1007/s42823-020-00224-z.

[35] C. Tsai and W. Tsai, "Optimization of physical activation process by CO_2 for activated carbon preparation from Honduras Mahogany Pod Husk," *Materials*, vol. 16, no. 19, 6558, pp. 1–11, 2023, doi: 10.3390/ma16196558.